Laser Control of Ion/Atom–Molecule Interaction: Application to ($X + CH_4$, $X = Li^+$ and Li) Reactions

Hassan Talaat,[1] El-Wallid S. Sedik,*[2] and M. Tag El-Din Kamal[2]

[1]Department of Physics, Faculty of Science, Ain Shams University, Cairo, Egypt

[2]Department of Theoretical Physics, National Research Center, Dokki, Giza, Egypt

Received April 30, 2009; E-mail: wsedik@yahoo.com

Laser atom/ion–molecule reaction interaction through dipole moments leads to potential energy surface crossings in ion molecule ($Li^+ + CH_4$) and barrier reshaping in atom–molecule reaction ($Li + CH_4$). We will show here by using gauge representation (electric field gauge) that we can create laser-induced surface crossing in the region (4 au) where the dipole moment changes sign for the $LiH + CH_3^+ \rightleftarrows Li^+ + CH_4$ reaction and reshape the barrier height (increase/decrease the height) by changing the laser phase for $Li + CH_4 \rightarrow LiH + CH_3$ where dipole moment changes sign in the transition state region.

Laser control and manipulation of reaction paths in molecular systems can lead to coherent control of the reaction path as a function of the absolute phase of an incident laser field through inclusion of dipole moments along the reaction path, thus leading to the potential surface crossings along the reaction path.

Molecular systems have permanent dipole moments which will interact with laser fields creating surface crossings. Infrared (IR) laser-induced chemical reactions were examined earlier by classical models where it was found that intense lasers will lower activation energies.[1] A quantum mechanical approach was used to show that barrier suppression[2] and modification of non adiabatic effects[3] is a general phenomenon in the presence of intense IR laser fields.

Crossing of potential energy surfaces is important in ion–molecule reactions as well as in charge-transfer processes, also barrier reshaping is important in atom–molecule reactions. In the present work we focus on the $Li^+ + CH_4$ ion–molecule and $Li + CH_4$ atom–molecule reaction with the goal of studying the effect of an intense laser field on the permanent dipole moment of this and other similar systems.[4] Using ab initio methods, we calculate the energy of the reaction path, and the permanent dipole moment along the reaction path. We restrict ourselves to a 1-D model using the electric field gauge representation of laser molecule interactions. This allows incorporation of the laser interaction directly into the potential surface, thus leading to simple analytic formulae to describe the laser-reaction path interactions. The second section explains the theory that shows potential surface crossing and barrier reshaping. The third section explains the ab initio calculation with the basis set used. The fourth section demonstrates the results and discussion for the atom/ion laser molecule interaction. The last section is the conclusion.

Theoretical Background

Laser Atom/Ion–Molecule Interaction. The standard description of laser-particle interaction starts from the classical electric-field particle interaction which by successive unitary transformations on the molecular time-dependent Schrödinger equation, TDSE, leads to various representations (gauges),[5] where particle radiative couplings have different frequency dependencies.[6] Since we shall consider 1-D reaction paths with coordinates $-\infty \le s \le \infty$, the corresponding TDSE with linear dipole moment $\mu(s) = \mu_o s$ can be written as:

$$i\frac{\partial\psi(s,t)}{\partial t} = \hat{H}\psi(s,t) = \left[\frac{p_s^2}{2m_s} + V(s) \pm \mu(s)\varepsilon(t)\right]\psi(s,t) \quad (1)$$

$\psi(s, t)$ is the wave function for propagation of the relative motion of a nuclear wave packet as a function of time along the reaction coordinate s which defines a potential $V(s)$ to be calculated by ab initio methods.

Charged particles of mass M_p subjected to long wavelength intense laser light undergo light-induced oscillations. The potential energy surface crossing describes electronic motion before and after laser effect at fixed nuclear position, as a result they acquire a ponderomotive energy[7,8] which is the oscillatory energy acquired by the particle during its propagation in the oscillatory electromagnetic field defined as,

$$U_p(\text{au}) = \frac{e^2E_o^2}{4M_p\omega^2} = \frac{3.4\times10^{-21}I(\text{W/cm}^2)\lambda^2(\text{nm})}{M_p/m_e} \quad (2)$$

where m_e is the mass of an electron. The turning point of the light induced oscillations are called ponderomotive radii,

$$\gamma_o(\text{au}) = \frac{2.4\times10^{-12}[I(\text{W/cm}^2)]^{1/2}\lambda^2(\text{nm})}{M_p/m_e} \quad (3)$$

for an intensity $I = cE_o^2/8\pi$ and wavelength λ. Clearly the influence of intense long wavelength laser fields will be strongest for the lightest ions such as H^+ and Na^+.

The system under investigation will be the ion–molecule reaction[9,10] and/or the reverse,[11–14]

$$LiH + CH_3^+ \leftrightarrow Li^+ + CH_4 \quad (4a)$$

$$Li + CH_4 \rightarrow LiH + CH_3 \quad (4b)$$

Published on the web May 15, 2010; doi:10.1246/bcsj.20090114

Thus in the center of mass system the reduced mass m_s will be nearly constant due to the much smaller mass of the transferred proton. The ab initio calculations below will show that the dipole moment of reaction (2) is indeed linear with s in the case of ion–molecule so that eq 1 with m_s constant will be an excellent approximation to represent the motion along the reaction path s in the presence of a laser field $\varepsilon(t) = E_o \cos \omega t$, with amplitude E_o and frequency ω. The laser–particle interaction in (1) is written in the dipole approximation $(s/\lambda) \ll 1$, i.e., the long wavelength approximation where λ is the wavelength of the laser field. As an example current intense near IR lasers operate at 800 nm whereas our simulations will be in the range $|s| \leq 1$ nm.

We shall be studying detailed variations of the potential surface $V(s)$, dipole moment $\mu(s)$, and polarizability $\alpha(s)$, along the reaction path s for $Li^+ + CH_4$. In the presence of strong fields of amplitude $\varepsilon(t) = E_o \cos(\omega t + \phi)$, where E_o is the maximum amplitude, ω the frequency, and ϕ the phase, high order radiative interactions will distort the surfaces. Nevertheless, an upper limit to the strength of the field is necessary in order to avoid ionization. In IR long wavelength fields, electronic ionization can be treated as a tunneling model.[15] Thus, using direct current (DC) tunneling theory,[16] one can estimate the tunneling ionization rate $w(t)$ for a static electric field amplitude E,[17]

$$w(t) = 4\omega_o \left[\frac{E_i}{E_h}\right]^{5/2} \frac{E_a}{\varepsilon(t)} \exp\left[-\frac{2}{3}\left[\frac{E_i}{E_h}\right]^{3/2} \frac{E_a}{\varepsilon(t)}\right] \quad (5)$$

where ω_o is the atomic frequency unit ($\omega_o = 4 \times 10^{16}\,s^{-1}$), E_h and E_i are the ionization potentials of hydrogen and the atom in question and E_a is the atomic unit of the electric field.

Below this threshold, nonlinear interactions with the electric field will occur, leading to a general dipole moment expression:

$$\mu = \mu_o + \frac{1}{2}\alpha\varepsilon + \frac{1}{6}\beta\varepsilon^2 + \frac{1}{24}\gamma\varepsilon^3 + \ldots \quad (6)$$

where μ_o is the permanent dipole moment, α the polarizability tensor, and β and γ are the first and second hyperpolarizability tensors. The essential parameters for the theoretical description of the alignment of molecules in the non resonant case are μ_o and α for intensities not exceeding $I = 3 \times 10^{13}\,W\,cm^{-2}$. Beyond this intensity, the hyperpolarizability expansion fails for the hydrogen atom whereas below this intensity, contributions from β and γ are negligible. We conclude from this that at intensities below $3 \times 10^{13}\,W\,cm^{-2}$ in the IR region, ionization is negligible and the field-perturbative expansion eq 6 for the total dipole moment is adequate up to the second term $\frac{1}{2}\alpha\varepsilon$, i.e., including only polarizability.

Having established the limits of applicability of perturbative approaches to laser–molecule interaction, we describe the laser–molecule Hamiltonian by retaining only the dipole $\mu(s)$ along the reaction path s, following[10,17–21]

$$\hat{H}_L = -\mu(s)\varepsilon(t)\cos\theta \quad (7)$$

assuming that the orientation term $\cos(\theta) = 1$, where the laser field is parallel to the molecular axis, assuming $\varepsilon(t) = E_o \cos(\omega t + \phi)$ for a circular polarized electric field (as shown later $\mu(s)$ will dominate at the transition state $s = 0$), we can rewrite eq 7 as:[15,16,21–24]

$$\hat{H}_L = -\mu(s)E_o \cos(\omega t + \phi) \quad (8)$$

θ and ϕ are respectively the polar and azimuthal angles of the molecular axis with respect to the laser field polarization vector.

Thus, the parameters $\mu(s)E_o$ determine the relative amplitude in the present case and ϕ remains the relative phase in eq 7. This creates periodic but non-symmetric electric fields which induce asymmetric concomitant dissociation and ionization. In the present work we will examine the effect of the laser fields on the reaction path based on eq 7 which will be dominant in the transition state region. It is to be noted immediately that for negative dipoles μ, destructive interferences will occur at some phase ϕ. We will examine the quasi-static low frequency limit and choose the instantaneous period $\omega t = 0$, so that the effective potential along the reaction path is defined as:[25–28]

$$V = V(s) - \mu(s)E_o \cos(\phi) \quad (9)$$

The parameters $\mu(s)$ are next calculated by ab initio methods in order to illustrate the laser–molecule interaction along the reaction path, based on eq 9 and this will be shown to be the dominant interaction in the transition state region.

Computational Methods

All calculations were carried out using the unrestricted second-order Møller–Plesset perturbation theory[29] including excitations from inner shell electrons and using a large polarized basis set supplemented with diffuse functions on all atoms [UMP2(full)/6-311++G(2d,2p)]. All geometry optimizations, potential energy scans, and reaction path tracings, were also carried out at the same computational level. Geometry optimizations carried out in this work are full unconstrained energy minimizations with respect to all geometric parameters.

Our optimization using the much larger basis set results in a linear C_{3v} transition structure and correct values for the dipole moment. Electronic structure calculations were performed using the Gaussian 2003 program.[30] Very tight convergence criteria for both the self-consistent field (SCF) calculation as well as for geometry optimizations were set in all calculations. We have used a large but rather coarse grid (of 0.15 Å step size on each coordinate axis). The calculation steps 6 points in mass-weighted internals in the forward direction and 6 points in the reverse direction, in steps of $0.1\,amu^{1/2}$ Bohr along the path. To determine the dipole moment of each reacting system at every point along the reaction path, a separate single point calculation had to be carried out using the optimized geometry from the calculation. The default electric field step size was specified by Gaussian 2003 (the electric field is increased in steps of 0.0001 au). The spin contamination was found to be negligible along the reaction paths.

Results and Discussion

An inverted repulsive Morse potential was fitted to the ab initio potential Figure 1a and $V(s)$ was obtained by ab initio quantum chemical calculations using configuration interaction at the level of MP2 which is described in the previous section. The potential smoothly fitted to the asymptotic energies of reactants $LiH + CH_3^+$ at $s = 0$ and products $Li^+ + CH_4$ at $s = 11$ au where s is the reaction coordinate. In Figure 1b

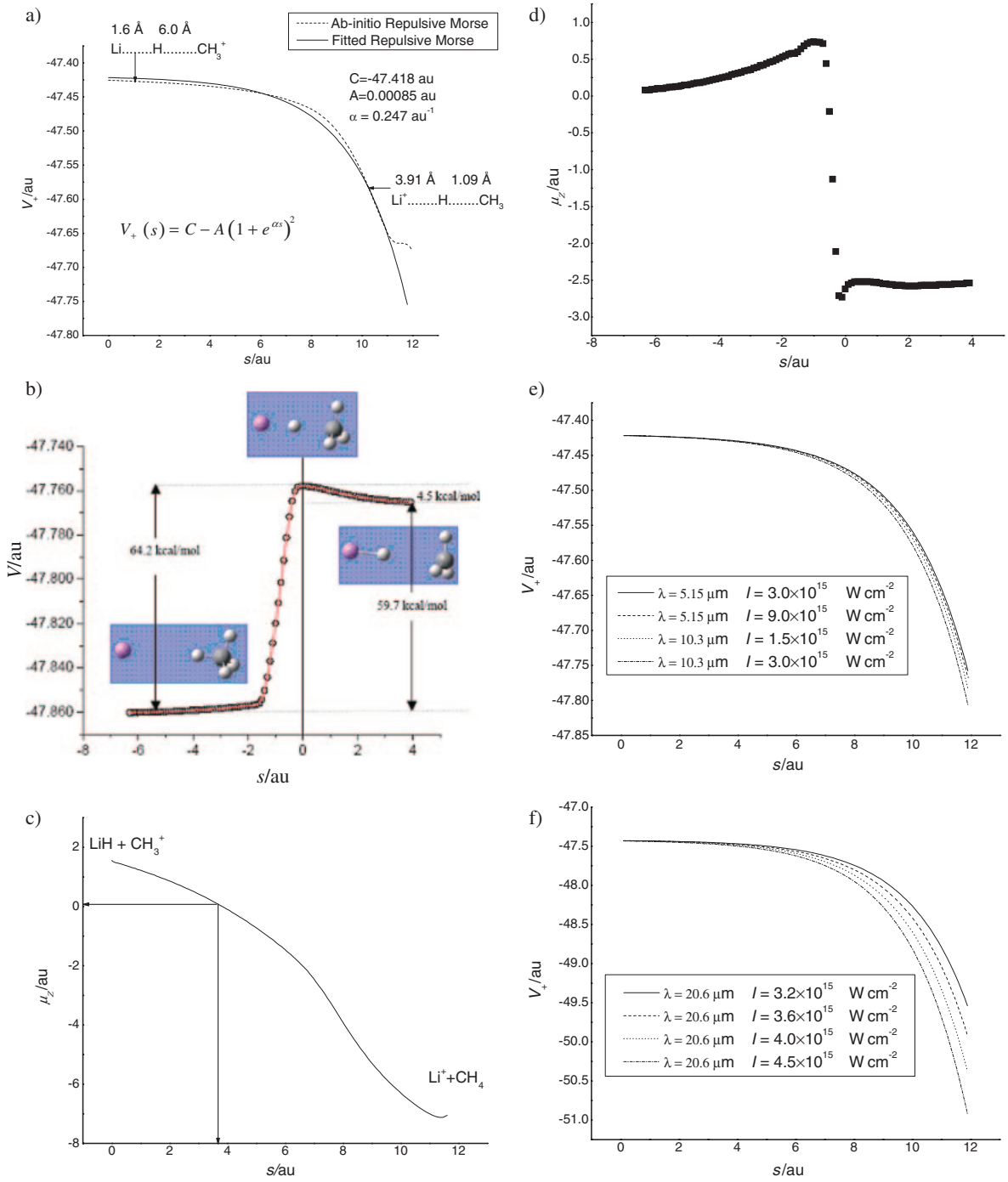

Figure 1. Plot of the potential energy surface of the $LiH + CH_3^+ \rightarrow Li^+ + CH_4$ reaction: a) repulsive inverted Morse (It is notable that the reaction lacks a transition state and the reaction proceeds without barrier to form the products.), b) plot of the potential energy surface of the $Li + CH_4 \rightarrow LiH + CH_3$ reaction reactants $Li + CH_4$ at -6.5 au and products $LiH + CH_3$ at 4 au, c) linear dipole moment for $Li^+ + CH_4$ reaction, d) the dipole moment for $Li + CH_4$ changes sign at the transition state region, and e), f) effect of laser on potential surface using the space translation gauge.

shows the reaction path for $Li + CH_4 \rightarrow LiH + CH_3$, reactants $Li + CH_4$ at -6.5 au and products $LiH + CH_3$ at $s = 4$ au. Figure 1c illustrates the ab initio permanent dipole moment $\mu(s)$ of the reactions (4a) along the reaction coordinate s. It is to be noticed that the dipole moment is nearly linear and $\partial\mu(s)/\partial s \cong -1$ au for $Li^+ + CH_4$ Figure 1d. The dipole moment for $Li + CH_4$ reaction (4b) changes sign at the transition state. Figures 2a and 2b shows the 2D inverted Morse for Li^+ in which the cationic system lacks a transition state and Li which has a transition state respectively.

In the case of the reaction $X = Li^+$, the reaction proceeds without a barrier although it posses a "virtual" transition state due to maximum polarizability which implies electron delocalization in the transition state. The reaction $LiH + CH_3^+$ starts

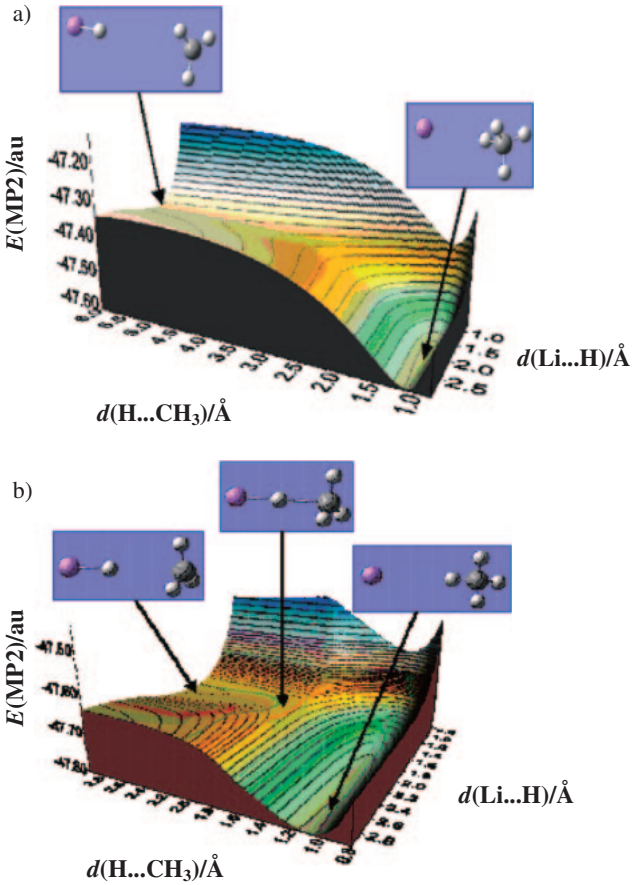

Figure 2. a) 2D potential energy surface of the $LiH + CH_3^+ \rightarrow Li^+ + CH_4$ reaction. The cationic system lacks transition state. b) 2D potential energy surface of the $LiH + CH_3 \rightarrow Li + CH_4$ reaction, the surface has a transition state.

at 0 au until it reaches 4 au at the virtual transition state and the product $Li^+ + CH_4$ is then formed at 12 au. The dipole moment for the ion reaction is linear with the reaction path and this moment can vanish at critical distances while for the atom–molecule reaction the dipole moment changes sign in the transition state region. This result implies maximum electron delocalization at this point along the reaction path.

For $Li + CH_4$ the reaction proceeds with a barrier. The reaction starts at -6.5 au until it reaches the product at 4 au. The dipole moment changes sign at the transition state. Barrier reshaping becomes possible (increase/decrease).

Electric field gauge is used to obtain the influence of the laser field on the potential surfaces of ion/atom–molecule systems. This leads to surface crossings/barrier reshaping respectively, Figures 3–6.

The present study shows as in Figures 3 and 4 the effect of the laser phase on molecules. The thick curve is the potential energy surface in the absence of the laser field while the thin curve is the potential energy surface in the presence of the laser field. In the intensity of $10^{12}\,W\,cm^{-2}$ controlling of the potential energy surface through laser phase was achieved at $\phi = 0$, the potential increases in height after it crosses the virtual transition state (4 au). By varying the laser phase

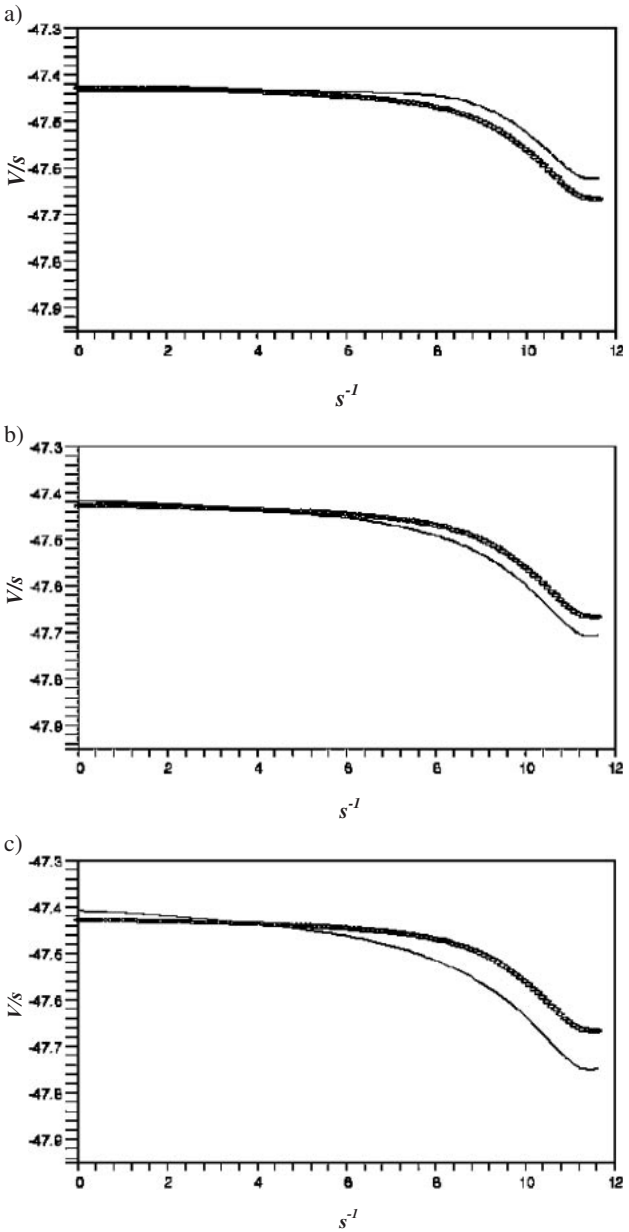

Figure 3. Snapshots of the energy profile along the reaction coordinate plus inclusion of only the dipole moment for $LiH + CH_3^+ \rightarrow Li^+ + CH_4$. $I = 5 \times 10^{12}\,W\,cm^{-2}$. a) $\phi = \pi/3$, b) $\phi = 2\pi/3$, and c) $\phi = \pi$.

$\phi = \pi/3$ we get a slight decrease in the height (0.05–0.1 au). Continuous variation of the laser phase leads to lowering of the potential at $\phi = 2\pi/3, \pi$.

In the intensity of $10^{13}\,W\,cm^{-2}$ controlling of the potential energy surface through laser phase was achieved at $\phi = 0$, the potential increases in height after it crosses at the virtual transition state (4 au). By varying the laser phase $\phi = \pi/3$ we get a slight decrease in the height (0.05–0.1 au). Continuous variation of the laser phase leads to lowering of the potential at $\phi = 2\pi/3, \pi$.

Figures 5 and 6 are for $Li + CH_4 \rightarrow LiH + CH_3$ in the intensity of $10^{12}\,W\,cm^{-2}$. The surface barrier decreases gradually in height at $\phi = 0$ and it continues its decrease at

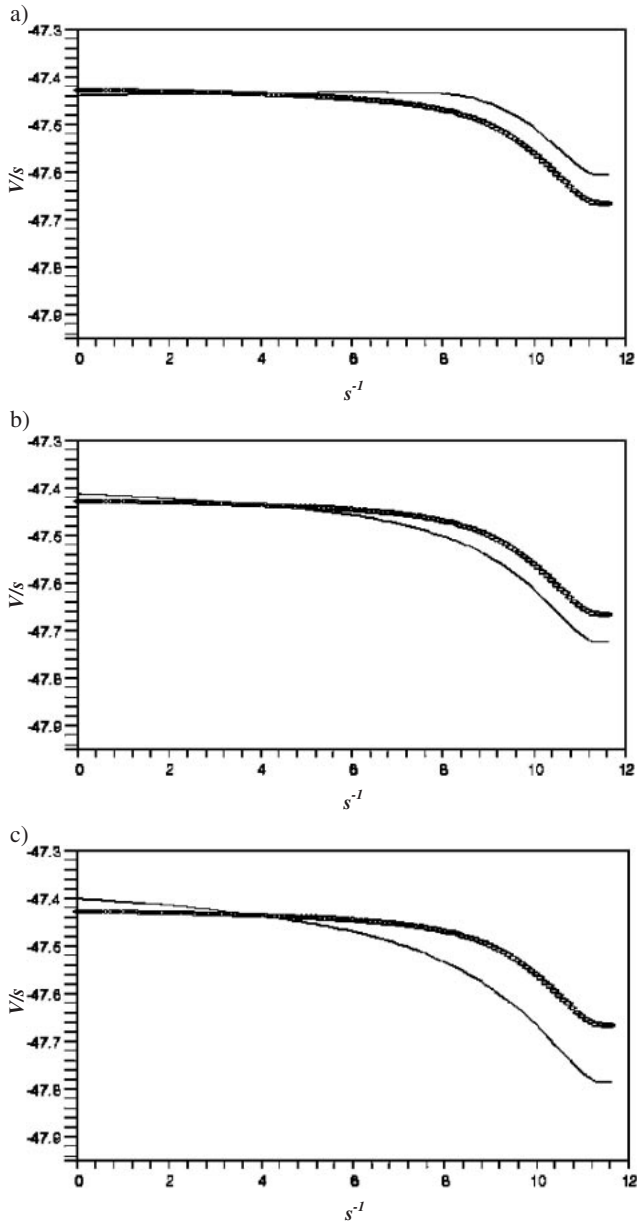

Figure 4. Snapshots of the energy profile along the reaction coordinate plus inclusion of only the dipole moment for $LiH + CH_3^+ \rightarrow Li^+ + CH_4$. $I = 1 \times 10^{13}\,W\,cm^{-2}$. a) $\phi = \pi/3$, b) $\phi = 2\pi/3$, and c) $\phi = \pi$.

$\phi = \pi/3$. Continuous variation of the laser phase leads to lowering and reshaping of the barrier at $\phi = 2\pi/3$, π. At the intensity of $10^{13}\,W\,cm^{-2}$ the surface barrier decreases gradually in height at $\phi = 0$ and it continues its decrease at $\phi = \pi/3$. Continuous variation of the laser phase leads to lowering and reshaping of the barrier at $\phi = 2\pi/3$, π.

The significance of our results is that the presence of an external electric field, be it time dependent as for a laser pulse or due to interfacial electric fields where polarity can be changed, maximum coupling with such phase-dependent external fields will occur at the transition state. Thus modification of the transition state is predicted to be controllable via the dipole and in the presence of a single laser field.

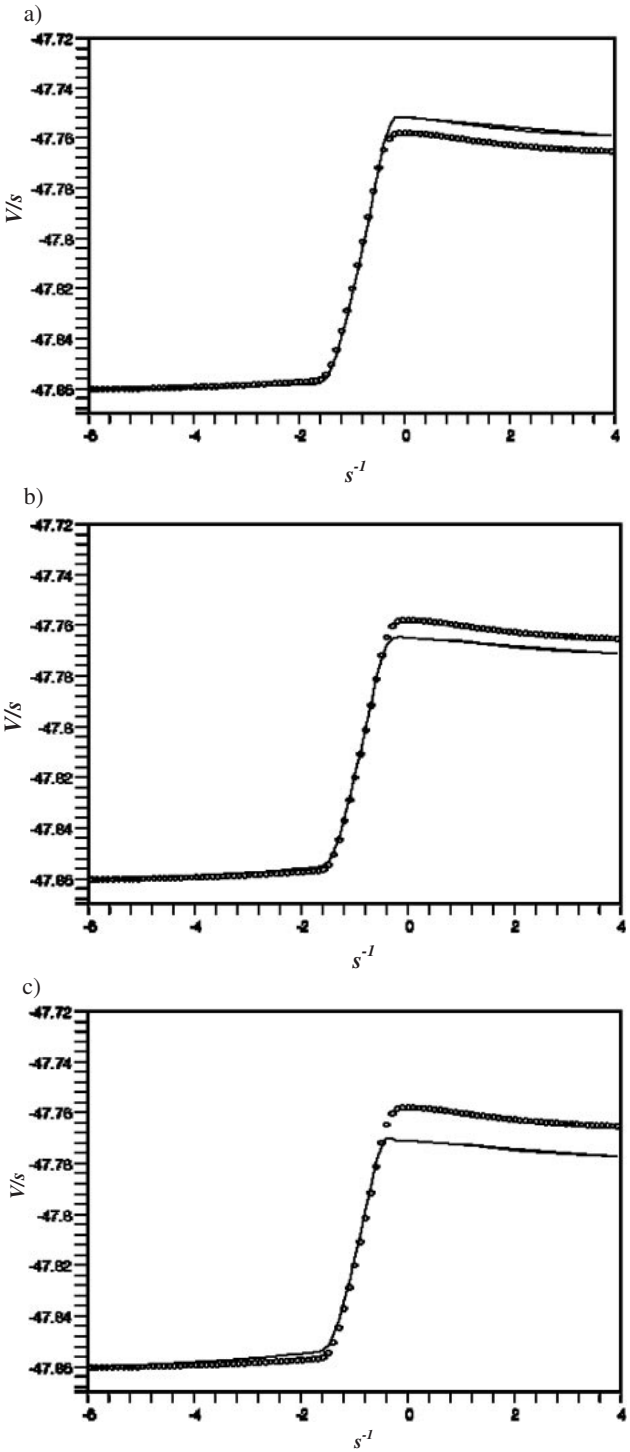

Figure 5. Snapshots of the energy profile along the reaction coordinate plus inclusion of only the dipole moment for $Li + CH_4 \rightarrow LiH + CH_3$. $I = 5 \times 10^{12}\,W\,cm^{-2}$. a) $\phi = \pi/3$, b) $\phi = 2\pi/3$, and c) $\phi = \pi$.

Current laser technology allows for the production of phase stabilized pulses for which the absolute phase is reproducible. What we have shown is that surface crossing and barrier reshaping will occur at high intensities (but below ionization thresholds) between permanent and laser-induced dipole moment effects, and these effects are maximum at the transition

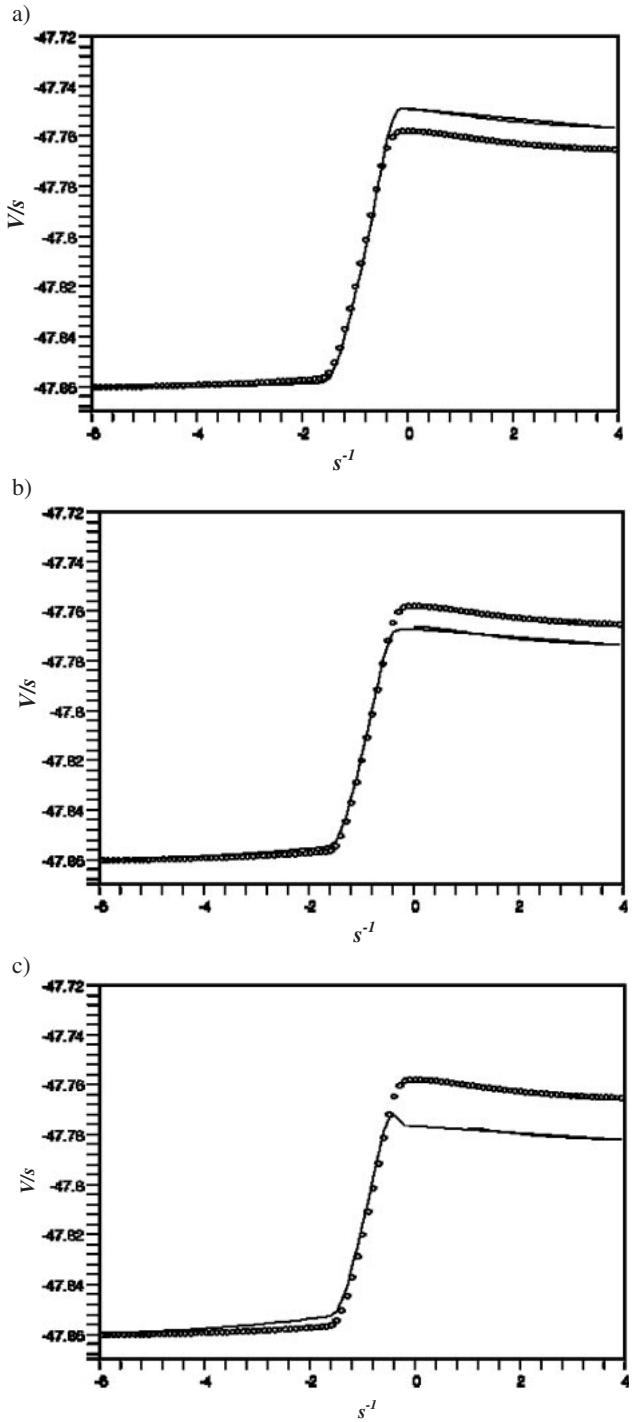

Figure 6. Snapshots of the energy profile along the reaction coordinate plus inclusion of only the dipole moment for $Li + CH_4 \rightarrow LiH + CH_3$. $I = 1 \times 10^{13}\,W\,cm^{-2}$. a) $\phi = \pi/3$, b) $\phi = 2\pi/3$, and c) $\phi = \pi$.

state. We have also demonstrated modifications to reaction rates and quantum tunneling in the presence of intense ultrashort IR laser fields below ionization threshold.

In the case of $Li^+ + CH_4 \rightarrow LiH + CH_3^+$ the reaction lacks a transition state by exposing it to IR laser field through the dipole moment and below threshold, we observe surface crossing due to the dipole moment changing sign in the virtual transition state where the polarizability is expected to be maximum. These crossings are important in ion–molecule reactions especially charge transfer.

In the case of $Li + CH_4 \rightarrow LiH + CH_3$ the reaction has a barrier by pointing an IR laser field the barrier height changes in the transition state which suggests reshaping of the barrier height and controlling the reaction probability.

Conclusion

We have studied the change in energetic and electric properties along the reaction paths of the ($X + CH_4$, $X = Li^+$ and Li) reactions, and linear transition states of C_{3v} symmetry were found for both reactions. We have added the laser–molecule interaction to the field free ab initio potentials using eq 9 for $\phi = \pi/3, 2\pi/3, \pi$ assuming $\omega t = 0$ and with an upper limit not exceeding $10^{13}\,W\,cm^{-2}$ to avoid ionization for both reactions. We found that for $Li^+ + CH_4$ that surface crossing becomes possible in the virtual transition state where dipole moment changes sign and the polarizability is expected to be maximum while for $Li + CH_4$, barrier reshaping becomes possible (increase/decrease) in barrier height which suggests control of chemical reactions.

The advent of phase stabilized near-femtosecond pulses should allow for observation of dipole contribution to the laser–molecule interaction at the transition state as predicted by eq 9, provided the duration of the pulse and collisional interaction at the transition state will be of comparable magnitude. One will expect alignment and therefore "guiding" of the reaction along the linear minimum energy path where the magnitude of the dipole moment are maximum as in the case of Li atom.

References

1 A. D. Bandrauk, H. Kono, in *Advances in Multiphoton Processes and Spectroscopy*, ed. by S. H. Lin, World Scientific, Singapore, **2003**, Vol. 15, p. 150.

2 M. Shapiro, P. Brumer, *Principles of the Quantum Control of Molecular Processes*, Wiley-Interscience, NY, **2003**.

3 G. Paulus, F. Lindner, H. Walther, A. Baltuška, E. Goulielmakis, M. Lezius, F. Krausz, *Phys. Rev. Lett.* **2003**, *91*, 253004.

4 V. S. Yakovlev, P. Dombi, G. Tempea, C. Lemell, J. Burgdörfer, T. Udem, A. Apolonski, *Appl. Phys. B* **2003**, *76*, 329.

5 F. Bloch, A. Nordsieck, *Phys. Rev.* **1937**, *52*, 54.

6 S. Chelkowski, A. D. Bandrauk, *Phys. Rev. A* **2002**, *65*, 061802.

7 C. A. S. Lima, L. C. M. Miranda, *Phys. Rev. A* **1981**, *23*, 3335.

8 R. M. O. Galvão, L. C. M. Miranda, *Phys. Rev. B* **1983**, *28*, 3593.

9 A. E. Orel, W. H. Miller, *Chem. Phys. Lett.* **1978**, *57*, 362; A. E. Orel, W. H. Miller, *J. Chem. Phys.* **1980**, *73*, 241.

10 A. D. Bandrauk, M. S. Child, *Mol. Phys.* **1970**, *19*, 95.

11 Ch. Zuhrt, T. Kamal, L. Zülicke, *Chem. Phys. Lett.* **1975**, *36*, 396.

12 J. C. Corchado, J. Espinosa-García, *J. Chem. Phys.* **1996**, *105*, 3160.

13 J. C. Corchado, J. Espinosa-García, *J. Chem. Phys.* **1996**, *105*, 3152.

14 J. C. Corchado, D. G. Truhlar, J. Espinosa-García, *J. Chem. Phys.* **2000**, *112*, 9375.
15 L. V. Keldysh, *Sov. Phys. JETP* **1965**, *20*, 1307.
16 P. B. Corkum, N. H. Burnett, F. Brunel, *Phys. Rev. Lett.* **1989**, *62*, 1259.
17 L. D. Landau, E. M. Lifshitz, *Quantum Mechanics*, Pergamon Press, NY, **1965**, p. 276.
18 A. E. Orel, W. H. Miller, *J. Chem. Phys.* **1979**, *70*, 4393.
19 T. Brabec, F. Krausz, *Rev. Mod. Phys.* **2000**, *72*, 545.
20 D. G. Truhlar, A. D. Isaacson, *J. Chem. Phys.* **1982**, *77*, 3516.
21 C. M. Dion, A. Keller, O. Atabek, A. D. Bandrauk, *Phys. Rev. A* **1999**, *59*, 1382.
22 V. Ramamurthy, J. Shailaja, L. S. Kaanumalle, R. B. Sunoj, J. Chandrasekhar, *Chem. Commun.* **2003**, 1987.
23 S. Chelkowski, A. D. Bandrauk, A. Apolonski, *Opt. Lett.* **2004**, *29*, 1557.
24 M. C. Heaven, in *Chemical Dynamics in Extreme Environments*, ed. by R. A. Dressler, World Scientific, Singapore, **2000**.
25 H. Stapelfeldt, T. Seideman, *Rev. Mod. Phys.* **2003**, *75*, 543.
26 L. Pan, K. T. Taylor, C. W. Clark, *J. Opt. Soc. Am. B* **1990**, *7*, 509.
27 A. D. Bandrauk, S. Chelkowski, *Phys. Rev. Lett.* **2000**, *84*, 3562.
28 J. Levesque, S. Chelkowski, A. D. Bandrauk, *J. Phys. Chem. A* **2003**, *107*, 3457.
29 C. Møller, M. S. Plesset, *Phys. Rev.* **1934**, *46*, 618.
30 M. J. Frisch, G. W. Trucks, H. B. Schlegel, G. E. Scuseria, M. A. Robb, J. R. Cheeseman, J. A. Montgomery, Jr., T. Vreven, K. N. Kudin, J. C. Burant, J. M. Millam, S. S. Iyengar, J. Tomasi, V. Barone, B. Mennucci, M. Cossi, G. Scalmani, N. Rega, G. A. Petersson, H. Nakatsuji, M. Hada, M. Ehara, K. Toyota, R. Fukuda, J. Hasegawa, M. Ishida, T. Nakajima, Y. Honda, O. Kitao, H. Nakai, M. Klene, X. Li, J. E. Knox, H. P. Hratchian, J. B. Cross, C. Adamo, J. Jaramillo, R. Gomperts, R. E. Stratmann, O. Yazyev, A. J. Austin, R. Cammi, C. Pomelli, J. W. Ochterski, P. Y. Ayala, K. Morokuma, G. A. Voth, P. Salvador, J. J. Dannenberg, V. G. Zakrzewski, S. Dapprich, A. D. Daniels, M. C. Strain, O. Farkas, D. K. Malick, A. D. Rabuck, K. Raghavachari, J. B. Foresman, J. V. Ortiz, Q. Cui, A. G. Baboul, S. Clifford, J. Cioslowski, B. B. Stefanov, G. Liu, A. Liashenko, P. Piskorz, I. Komaromi, R. L. Martin, D. J. Fox, T. Keith, M. A. Al-Laham, C. Y. Peng, A. Nanayakkara, M. Challacombe, P. M. W. Gill, B. Johnson, W. Chen, M. W. Wong, C. Gonzalez, J. A. Pople, *Gaussian 03, Revision B.03*, Gaussian Inc., Pittsburgh PA, **2003**.